Science Signaling
AAAS

` Ras Stabilization Through Aberrant Activation of Wnt/{beta}-Catenin Signaling Promotes Intestinal Tumorigenesis

Woo-Jeong Jeong, Juyong Yoon, Jong-Chan Park, Soung-Hoon Lee, Seung-Hoon Lee, Saluja Kaduwal, Hoguen Kim, Jong-Bok Yoon and Kang-Yell Choi (10 April 2012)

Science Signaling **5** (219), ra30. [DOI: 10.1126/scisignal.2002242]

The following resources related to this article are available online at http://stke.sciencemag.org.
This information is current as of 18 April 2012.

Article Tools Visit the online version of this article to access the personalization and article tools:
http://stke.sciencemag.org/cgi/content/full/sigtrans;5/219/ra30

Supplemental Materials *"Supplementary Materials"*
http://stke.sciencemag.org/cgi/content/full/sigtrans;5/219/ra30/DC1

Related Content The editors suggest related resources on *Science*'s sites:
http://stke.sciencemag.org/cgi/content/abstract/sigtrans;5/219/pe15
http://stke.sciencemag.org/cgi/content/abstract/sigtrans;5/206/ra3

References This article cites 42 articles, 23 of which can be accessed for free:
http://stke.sciencemag.org/cgi/content/full/sigtrans;5/219/ra30#otherarticles

Glossary Look up definitions for abbreviations and terms found in this article:
http://stke.sciencemag.org/glossary/

Permissions Obtain information about reproducing this article:
http://www.sciencemag.org/about/permissions.dtl

Downloaded from stke.sciencemag.org on April 18, 2012

Science Signaling (ISSN 1937-9145) is published weekly, except the last week in December, by the American Association for the Advancement of Science, 1200 New York Avenue, NW, Washington, DC 20005. Copyright 2008 by the American Association for the Advancement of Science; all rights reserved.

CANCER

Ras Stabilization Through Aberrant Activation of Wnt/β-Catenin Signaling Promotes Intestinal Tumorigenesis

Woo-Jeong Jeong,[1,2]* Juyong Yoon,[1,2]* Jong-Chan Park,[1,2] Soung-Hoon Lee,[1,2] Seung-Hoon Lee,[1,3] Saluja Kaduwal,[1,2] Hoguen Kim,[4] Jong-Bok Yoon,[1,3] Kang-Yell Choi[1,2]†

Although the guanosine triphosphate/guanosine diphosphate loading switch is a major regulatory mechanism that controls the activity of the guanosine triphosphatase Ras, we report a distinct mechanism for regulating Ras activity through phosphorylation-mediated degradation and describe the role of this second regulatory mechanism in the suppression of cellular transformation and tumors induced by *Ras* mutations. We found that negative regulators of Wnt/β-catenin signaling contributed to the polyubiquitin-dependent degradation of Ras after its phosphorylation by glycogen synthase kinase 3β (GSK3β) and the subsequent recruitment of β-TrCP–E3 ligase. We found a positive association between tumorigenesis and Ras stabilization resulting from the aberrant activation of Wnt/β-catenin signaling in adenomas from two mouse models of colon cancer, human colonic tumors from various stages, and colon polyps of patients with familial adenomatous polyposis. Our results indicated that GSK3β plays an essential role in Ras degradation and that inhibition of this degradation pathway by aberrant Wnt/β-catenin signaling may contribute to Ras-induced transformation in colorectal tumorigenesis.

INTRODUCTION

Three decades after the identification of *Ras* as an oncogene, the field remains a dynamic and active area of investigation. Studies have shown that Ras activates the mitogen-activated protein kinase (MAPK) pathway which controls diverse biological processes, including growth and the differentiation of cells, and Ras and the MAPK pathway have been implicated in a number of diseases, including cancer and certain developmental disorders. Oncogenic mutations in *Ras* have been reported in one-third of all human cancers; however, therapies directly targeting Ras have so far been unsuccessful (*1*–*3*).

There are three main Ras isoforms, H-Ras, K-Ras, and N-Ras, and the activity of these small guanosine triphosphatases (GTPases) is controlled by a guanosine diphosphate (GDP)/guanosine triphosphate (GTP) loading switch (*4*). Mutations that lock Ras into the active GTP-bound forms are major causes of human cancers (*2*, *5*). There is evidence to suggest that other mechanisms also regulate Ras activity, such as ubiquitylation (*6*) and differential activity through subcellular localization and the recruitment of different regulators of Ras (*7*). The roles of these additional regulatory mechanisms in cancer are poorly understood. The E3 ligase substrate recognition protein β-TrCP contributes to H-Ras degradation (*8*). H-Ras is also subject to mono- and di-ubiquitylation, and these posttranslational modifications affect the cellular trafficking of H-Ras (*6*); how this influences H-Ras activity and the physiological relevance of this modification is not clear.

Two key genetic events in the development of colon cancer are aberrant activation of the Ras-MAPK and Wnt/β-catenin signaling pathways (*9*). The Wnt/β-catenin pathway plays an important role in both oncogenesis and development (*10*). In a resting state, β-catenin interacts with the destruction complex, including the scaffolding proteins adenomatous polyposis coli (APC) and Axin and the kinases casein kinase 1 (CK1) and glycogen synthase kinase 3β (GSK3β). GSK3β-phosphorylated β-catenin is recognized by β-TrCP and is subject to polyubiquitin-dependent proteasomal degradation (*11*, *12*). Regulation of β-catenin through degradation is a critical mechanism controlling its activity as a transcriptional regulator, affecting expression of target genes involved in cellular transformation and oncogenesis (*13*, *14*). The Ras–extracellular signal–regulated kinase (ERK) and Wnt/β-catenin pathways interact in the promotion of tumors (*15*–*18*). We previously found, using mainly in vitro studies, inhibition of the Ras-ERK pathway by inhibitors of Wnt/β-catenin pathway, such as APC and Axin, and reported that this regulation related with reduced proliferation (*19*, *20*). These studies indicated a potential mechanism for tumor promotion by mutational synergistic activation of the Wnt/β-catenin and Ras pathways. The ERK pathway inhibition through negative Wnt/β-catenin signaling occurred by proteasomal degradation of Ras mediated by β-TrCP–E3 ligase (*8*). However, the detailed mechanism, including molecular events triggering the recruitment of β-TrCP–E3 ligase to Ras, was not determined. GSK3β has also been implicated in regulating Ras-mediated oncogenesis through an unknown mechanism (*21*). Therefore, we explored how GSK3β controlled Ras-mediated oncogenesis and identified a mechanism by which Wnt signaling promoted the stabilization of Ras by inhibiting Ras phosphorylation by GSK3β. Furthermore, this pathway was associated with colorectal tumorigenesis, thus providing an additional mechanism for the formation of tumors involving Ras to the mechanism involving *Ras* mutations.

RESULTS

Axin stimulates GSK3β-mediated H-Ras degradation

In a previous study, H-Ras was recognized by β-TrCP (*8*). Because β-TrCP recognizes β-catenin phosphorylated by GSK3β (*11*, *12*), we investigated whether GSK3β phosphorylated H-Ras and contributed to its ubiquitylation. We detected all Ras isoforms present in human embryonic kidney

[1]Translational Research Center for Protein Function Control, Yonsei University, Seoul 120-749, Korea. [2]Department of Biotechnology, College of Life Science and Biotechnology, Yonsei University, Seoul 120-749, Korea. [3]Department of Biochemistry, College of Life Science and Biotechnology, Yonsei University, Seoul 120-749, Korea. [4]Department of Pathology, Center for Chronic Metabolic Disease, College of Medicine, Yonsei University, Seoul 120-749, Korea.
*These authors contributed equally to this work.
†To whom correspondence should be addressed. E-mail: kychoi@yonsei.ac.kr

Downloaded from stke.sciencemag.org on April 18, 2012

(HEK) 293 cells with an antibody that recognizes H-Ras, K-Ras, and N-Ras. The amount of endogenous Ras in HEK293 cells was increased or decreased by knockdown or overexpression of GSK3β, respectively. In contrast, the amount of endogenous Ras polyubiquitylation was decreased by GSK3β knockdown and increased by overexpression of GSK3β (Fig. 1A). To determine whether H-Ras was specifically stabilized in the absence of GSK3β, we monitored the abundance of Myc-tagged H-Ras in *Gsk3*β$^{-/-}$ murine embryonic fibroblast (MEF) cells that were treated with the de novo protein synthesis inhibitor cycloheximide (CHX). Myc-tagged H-Ras degradation was inhibited in *Gsk3*β$^{-/-}$ MEF cells treated with CHX, and H-Ras degradation was rescued by replacement of GSK3β (fig. S1A). We confirmed that GSK3β promoted endogenous Ras destabilization by showing that endogenous Ras degradation was blocked in *Gsk3*β$^{-/-}$ cells treated with CHX (fig. S1B).

To determine whether GSK3β functioned in the recruitment of β-TrCP, we tested the effect of a constitutively active form of GSK3β on the interaction between endogenous β-TrCP and Ras. The β-TrCP and Ras interaction was weak, but was enhanced by overexpression of catalytically active GSK3β (GSK3βCA) (Fig. 1B). The abundance of Myc-tagged H-Ras was increased by *Gsk3*β knockout, even in the presence of overexpressed β-TrCP. Enhanced H-Ras degradation in cells overexpressing β-TrCP was completely abolished in *Gsk3*β$^{-/-}$ cells and was rescued by the reintroduction

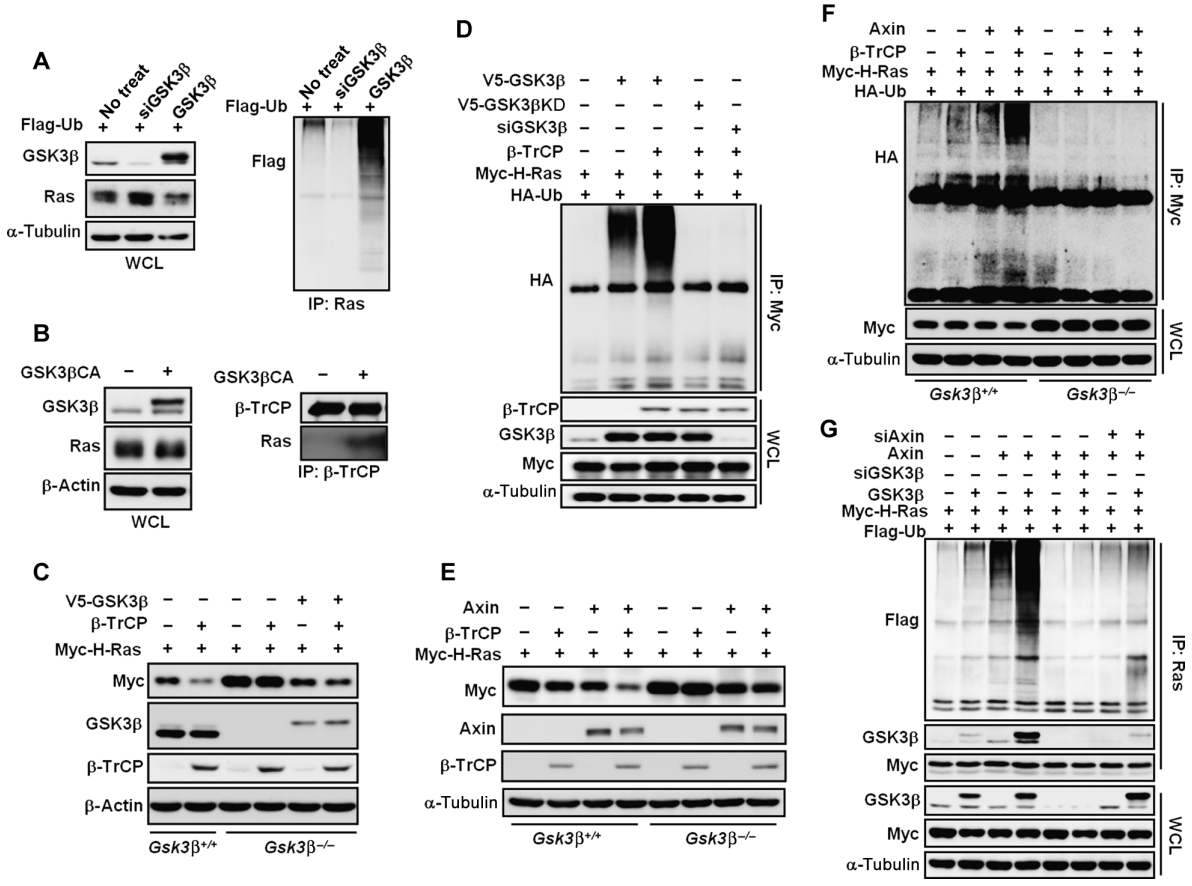

Fig. 1. Axin enhances GSK3β-mediated degradation and polyubiquitylation of H-Ras. (**A**) Effects of the knockdown or overexpression of GSK3β on the stability and ubiquitylation of H-Ras. HEK293 cells were transfected with the indicated vectors [siRNA (siGSK3β); overexpression (GSK3β); control Flag-tagged ubiquitin only (no treat)], and whole-cell lysates (WCLs) were immunoblotted for the indicated proteins. Samples on the right represent WCLs immunoprecipitated with an antibody that recognizes all Ras isoforms (anti-Ras) from cells treated with the proteasome inhibitor ALLN and then blotted with the antibody recognizing Flag-tagged ubiquitin. Data are representative of two experiments. (**B**) Effect of GSK3β activation on the interaction between endogenous β-TrCP and Ras. HEK293 cells were transfected with catalytically active GSK3β (GSK3βCA) and then treated with ALLN. WCLs were immunoprecipitated with an antibody recognizing β-TrCP and blotted with antibodies to the indicated proteins. Data are representative of three experiments. (**C**) Effects of knockout or replacement of GSK3β on H-Ras stability. *Gsk3*β$^{+/+}$ or *Gsk3*β$^{-/-}$ MEF cells were transfected with the indicated vectors, and WCLs were immunoblotted for the indicated proteins. Data are representative of two experiments. (**D**) Effects of knockdown or overexpression of wild-type (V5-GSK3β) or kinase-defective GSK3β (V5-GSK3βKD) on the polyubiquitylation of H-Ras enhanced by overexpression of β-TrCP. HEK293 cells were transfected with the indicated vectors and then treated with ALLN. WCLs were then immunoprecipitated with an antibody recognizing Myc. (**E** and **F**) Effects of GSK3β knockout on the enhancement of β-TrCP–mediated degradation and polyubiquitylation of H-Ras by Axin. *Gsk3*β$^{+/+}$ or *Gsk3*β$^{-/-}$ cells were transfected with the indicated vectors and then analyzed (E) or treated with ALLN (F). Proteins were immunoprecipitated with antibody recognizing Myc. (**G**) The effect of GSK3β knockdown with or without Axin knockdown on Ras ubiquitination. HEK293 cells were transfected with the indicated vectors and then treated with ALLN. WCLs were immunoprecipitated with the anti-Ras antibody. IP, immunoprecipitation.

Downloaded from stke.sciencemag.org on April 18, 2012

of GSK3β into the cells (Fig. 1C). Expression of a kinase-defective GSK3β (GSK3βKD) mutant stabilized H-Ras (fig. S1C), indicating that GSK3β kinase activity was essential for H-Ras degradation. Moreover, GSK3β overexpression increased H-Ras polyubiquitylation [detected in cells treated with the proteasome inhibitor *N*-acetyl-leucinyl-leucinyl-norleucinal (ALLN)], which was further increased by coexpression of β-TrCP. H-Ras polyubiquitylation by β-TrCP was barely detectable in cells overexpressing GSK3βKD or cells in which GSK3β was knocked down with short interfering RNA (siRNA) (Fig. 1D). Together, these results suggest that H-Ras polyubiquitylation and degradation by β-TrCP are tightly associated with GSK3β activity.

Because Axin is a negative regulator of Wnt signaling and a component of the β-catenin destruction complex that also includes GSK3β, we investigated whether Axin contributed to GSK3β-mediated Ras degradation by monitoring H-Ras abundance in *Gsk3*$\beta^{+/+}$ and *Gsk3*$\beta^{-/-}$ cells, in response to overexpression or knockdown of Axin1. In *Gsk3*$\beta^{+/+}$ cells, but not *Gsk3*$\beta^{-/-}$ cells, coexpression of both β-TrCP and Axin reduced the abundance of H-Ras (Fig. 1E). H-Ras polyubiquitylation in *Gsk3*$\beta^{+/+}$ cells, but not in *Gsk3*$\beta^{-/-}$ cells, was increased in cells coexpressing β-TrCP and Axin in both nondenaturing and denaturing conditions (Fig. 1F and fig. S1D). The role of GSK3β and Axin in regulating Ras stability was further demonstrated by the reduction in the abundance of endogenous Ras in response to overexpression of these two proteins and the reversal of these effects by treatment with the GSK3β inhibitor LiCl (fig. S1E).

To investigate the mechanism by which Axin promoted the destabilization of Ras, we monitored the effect of Axin overexpression or knockdown on the interaction between GSK3β and Ras. The amount of H-Ras polyubiquitylation correlated with the amount of GSK3β that coimmunoprecipitated with H-Ras; the greatest amount of polyubiquitylation and interaction occurred in cells overexpressing both Axin and GSK3β (Fig. 1G). The enhancement of the GSK3β-Ras interaction and H-Ras polyubiquitylation by overexpressed Axin was negated by knockdown of GSK3β or Axin (Fig. 1G). To determine whether the interaction between Axin and GSK3β was important for the polyubiquitylation and destabilization of Ras, we monitored the effects of Axin1$^{\Delta Ex4\text{-}5}$, an Axin mutant that lacks the domain needed for binding GSK3β (fig. S1F) (*22*). The enhanced degradation and polyubiquitylation of H-Ras, as well as the interaction between H-Ras and GSK3β, were absent in cells overexpressing Axin1$^{\Delta Ex4\text{-}5}$ (fig. S1, G and H). Thus, Axin appears to serve as a bridge enabling GSK3β-mediated polyubiquitylation and degradation of H-Ras.

Phosphorylation is essential for H-Ras degradation

In vitro kinase assays with purified recombinant H-Ras and GSK3β showed that histidine-tagged H-Ras (His–H-Ras) was phosphorylated by GSK3β (Fig. 2A). We confirmed this phosphorylation event with an immunocomplex kinase assay, using the constitutively active GSK3β mutant (GSK3βCA) or the catalytically inactive mutant GSK3βKD. His–H-Ras was phosphorylated in the presence of immunopurified GSK3βCA, but not in the presence of GSK3βKD (Fig. 2B).

Because β-TrCP functions as a component of the Skp1–Cul1–F-box protein (SCF) E3 ubiquitin ligase, we analyzed whether SCF$^{\beta\text{-TrCP}}$ functioned as a ubiquitin ligase for H-Ras in vitro and whether this process required phosphorylation of H-Ras by GSK3β. H-Ras was ubiquitylated by SCF$^{\beta\text{-TrCP}}$ ubiquitin ligase complex in vitro, and this process was enhanced by H-Ras phosphorylation by GSK3β (Fig. 2C). Liquid chromatography–tandem mass spectrometry (LC-MS/MS) analysis of the in vitro–phosphorylated H-Ras band revealed phosphorylation at Thr^{144}, Thr^{148} (Fig. 2D), and Ser^{183} (fig. S2A). However, degradation of an H-Ras mutant lacking the hypervariable region (H-Ras–ΔHVR), which includes Ser^{183}, was enhanced by coexpression of β-TrCP and Axin in *Gsk3*$\beta^{+/+}$ cells (fig. S2B), suggesting that phosphorylation at this residue does not contribute to β-TrCP–mediated degradation of H-Ras. In contrast, the Thr^{144} and Thr^{148} residues of H-Ras are located in a GSK3β phosphorylation consensus motif, S/TXXXS/T (fig. S2C) (*23*, *24*), and these amino acids (^{144}TSAKT^{148}) are also conserved in other Ras isoforms (fig. S2B). Consistent with this regulatory mechanism for degradation occurring for other Ras isoforms, we found that the amount of Myc-tagged K-Ras and Myc-tagged N-Ras was increased in *Gsk3*$\beta^{-/-}$ cells compared with the amount of these proteins in *Gsk3*$\beta^{+/+}$ cells (Fig. 2E). Cells transfected to express K- or N-Ras also exhibited ubiquitylation and reduced stability in cells overexpressing β-TrCP that was independent of the HVR (fig. S3). Thus, we focused on the role of the Thr^{144} and Thr^{148} residues in H-Ras destabilization.

We generated phosphorylation-deficient (T144A/T148A; H-Ras-2A) and phosphorylation-mimetic (T144E/T148E; H-Ras-2E) mutants. We confirmed that His–H-Ras-2A was not phosphorylated by GSK3βCA (Fig. 2B). Although wild-type H-Ras expressed with GSK3β exhibited a half-life of 6 hours, H-Ras-2A expressed with GSK3β was stable (fig. S4A). To study the role of phosphorylation in regulating H-Ras stability, we generated a polyclonal antibody recognizing phosphorylated H-Ras (p-H-Ras) that did not recognize either H-Ras mutant, H-Ras-2A or H-Ras-2E (fig. S4B). The abundance of p-H-Ras in cells that express wild-type H-Ras or in cells that express an oncogenic mutant form of H-Ras (H-Ras^{L61}) was increased by overexpression of GSK3β (Fig. 2F). In cells expressing Myc-tagged H-Ras, the abundance of p-H-Ras was also increased by overexpression of Axin, but the increase in the abundance of this phosphorylated form resulting from overexpression of GSK3β and Axin was abolished by exposure of the cells to Wnt3a, which inhibits GSK3β activity (Fig. 2G).

We assessed the importance of the two phosphorylation sites in H-Ras for β-TrCP–induced degradation in *Gsk3*$\beta^{+/+}$ and *Gsk3*$\beta^{-/-}$ cells (Fig. 2H). When the T144A/T148A mutation was made in the context of wild-type or oncogenic H-Ras^{L61}, overexpression of β-TrCP failed to promote the degradation of either form of H-Ras-2A. Conversely, H-Ras-2E appeared unstable and was further degraded after the transfection with β-TrCP in either *Gsk3*$\beta^{+/+}$ or *Gsk3*$\beta^{-/-}$ cells, whether phosphomimetic substitution was constructed in wild-type or oncogenic H-Ras (Fig. 2H and fig. S4C). Transcript abundance was similar for wild-type, H-Ras-2A, and H-Ras-2E, suggesting that the differences in abundance of these proteins in the transfected cells were not due to differences in expression (fig. S4D). Analysis of the half-life of H-Ras-2A and H-Ras-2E in cells treated with CHX to inhibit protein synthesis showed that H-Ras-2E had the shortest half-life in cells overexpressing β-TrCP and that H-Ras-2A was stable (fig. S4E).

To identify the role of phosphorylation in H-Ras ubiquitination, we qualitatively analyzed the polyubiquitylation of H-Ras phosphorylation mutants. H-Ras-2A exhibited the least, and H-Ras-2E exhibited the most, GSK3β and β-TrCP–mediated polyubiquitylation, and the relative amount of polyubiquitylation correlated with the coimmunoprecipitated β-TrCP (Fig. 2I). The apparent increase in wild-type H-Ras polyubiquitylation and phosphorylation induced by overexpression of β-TrCP and GSK3β was blocked by treatment of the cells with recombinant Wnt3a, and this inhibition was associated with reduced coimmunoprecipitation of β-TrCP. These data indicated that Wnt/β-catenin signaling stabilized Ras, whereas blocking Wnt/β-catenin signaling by overexpressing Axin destabilized Ras through a mechanism involving GSK3β-mediated phosphorylation of H-Ras at Thr^{144} and Thr^{148} and recruitment of the E3 ligase linker protein β-TrCP.

Phosphorylation-mediated H-Ras degradation inhibits ERK pathway activity

To determine the effect of Ras destabilization by GSK3β on the activation of the downstream ERK pathway, we monitored the effects of GSK3β on activation of the ERK pathway by oncogenic Ras or epidermal growth factor (EGF). Overexpression of GSK3β inhibited the increase in phosphorylated

Downloaded from stke.sciencemag.org on April 18, 2012

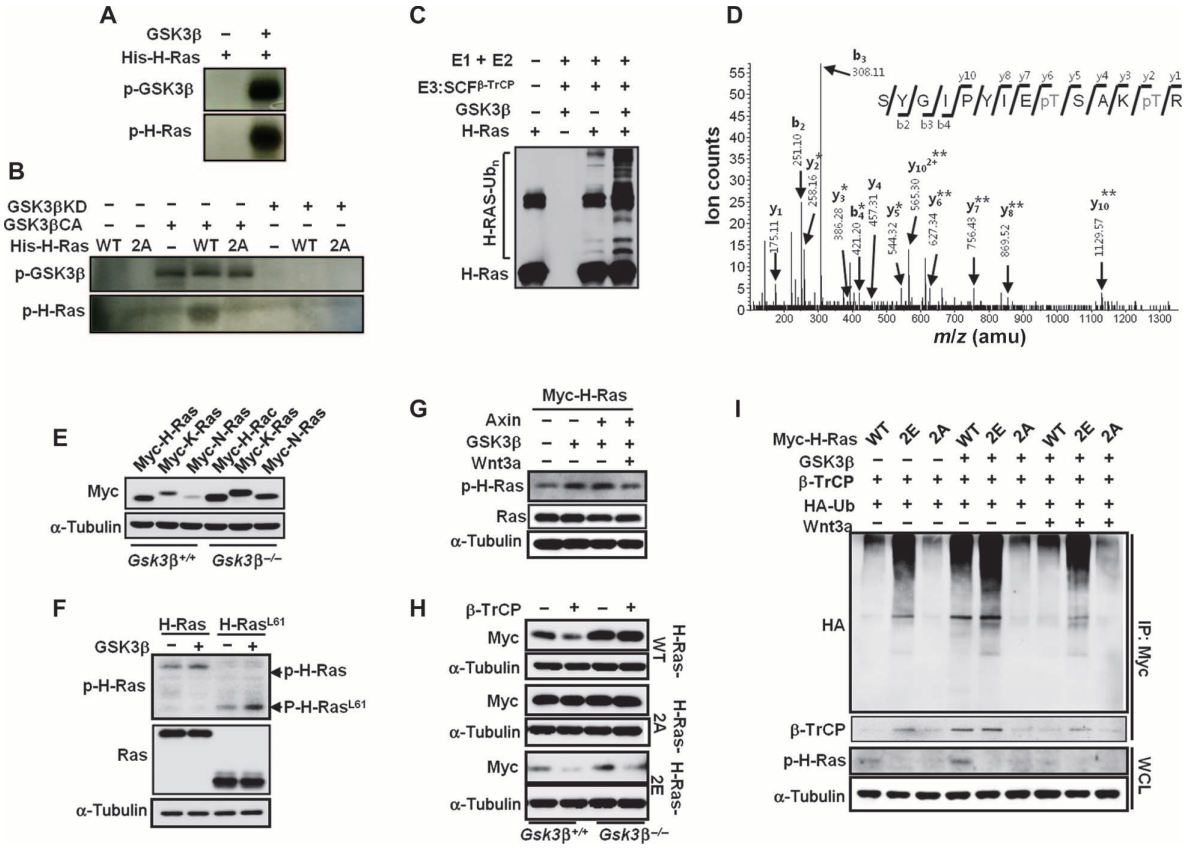

Fig. 2. Phosphorylation of H-Ras at Thr^{144} and Thr^{148} is related with polyubiquitylation and degradation. (**A**) In vitro kinase assay with His–H-Ras in the absence or presence of GSK3β. Data are representative of five experiments. (**B**) Immune complex kinase assays with immunopurified GSK3βCA or GSK3βKD together with His–H-Ras [wild-type (WT)] or His–H-Ras-2A (2A). Data are representative of two experiments. (**C**) H-Ras ubiquitylation by SCF$^{β\text{-TrCP}}$ is enhanced by GSK3β. Purified H-Ras was subjected to in vitro ubiquitylation by SCF$^{β\text{-TrCP}}$ complexes in the absence or presence of GSK3β. H-Ras was detected with the anti-Ras antibody. Data are representative of three experiments. (**D**) Electrospray ionization (ESI) tandem mass spectrum containing phosphorylated Ras-T^{144}/T^{148}. (**E**) Effects of GSK3β knockout on the stability regulation of H-, K-, and N-Ras. *Gsk3β*$^{+/+}$ or *Gsk3β*$^{-/-}$ cells were transfected with Myc-tagged H-Ras, Myc-tagged K-Ras, or Myc-tagged N-Ras. (**F**) Specific recognition of phosphorylated H-Ras or H-Ras^{L61} at Thr^{144} and Thr^{148} by a polyclonal rabbit antibody recognizing p-Ras. HEK293 cells were transfected with the indicated constructs and then treated with ALLN. Data are representative of two experiments. (**G**) The effects of Wnt/β-catenin signaling on H-Ras phosphorylation. HEK293 cells were transfected with the indicated constructs and then treated with ALLN. Where indicated, Wnt3a was administered for 2 hours before harvesting. (**H**) Effects of phosphorylation-deficient or phosphorylation-mimetic mutations in H-Ras on protein stability. *Gsk3β*$^{+/+}$ and *Gsk3β*$^{-/-}$ cells were transfected with constructs indicated on the right with or without cotransfection with β-TrCP. Proteins were detected with antibodies recognizing the epitopes or proteins indicated on the left. Data are representative of two experiments. (**I**) Effects of phosphorylation-deficient and phosphorylation-mimetic mutations in the presence or absence of Wnt3a on the phosphorylation, ubiquitination, and β-TrCP–binding affinity of H-Ras. HEK293 cells were transfected with the indicated constructs, treated with ALLN and Wnt3a, and immunoprecipitated with an antibody recognizing Myc. Data are representative of two experiments.

ERK (p-ERK) and activating transcription factor 2 [Atf-2, a transcription factor targeted by ERK; (*25*)] and reduced Elk-1 reporter activity in response to oncogenic H-Ras^{L61} (Fig. 3, A and B) or EGF (fig. S5, A and B). In both cases, the reductions in ERK signaling were associated with reduced abundance of Ras in the GSK3β-overexpressing cells. Both short- and long-term ERK activation and Elk-1 reporter activation by EGF or oncogenic H-Ras^{L61} were inhibited in HEK293 cells expressing H-Ras-2E and were enhanced in cells expressing H-Ras-2A (Fig. 3, C and D, and fig. S5, C and D). To confirm that inhibition of ERK pathway activity was not the result of altered Ras trafficking, we assessed the localization of Ras with an antibody recognizing Ras or phosphorylated Ras (p-Ras). We found that both Ras and p-Ras localized at similar subcellular regions (fig. S6). Thus, regulation of the stability of both wild-type and oncogenic mutant H-Ras proteins by GSK3β affects signaling through the ERK pathway.

H-Ras phosphorylation suppresses proliferation and transformation

To investigate the importance of the phosphorylation and degradation of H-Ras in cellular proliferation and transformation, we monitored the effects of expressing the phosphorylation-deficient Ras mutant on proliferation and transformation. In this experiment, we used oncogenic H-Ras^{L61} because this mutant has been reported to be degraded by β-TrCP in a process involving Axin (*8*). The proliferation of *Gsk3β*$^{+/+}$ cells expressing H-Ras^{L61} but those expressing with H-Ras^{L61}-2A was reduced by overexpression of

Downloaded from stke.sciencemag.org on April 18, 2012

β-TrCP, Axin, or both. In contrast, proliferation of *Gsk3*β$^{-/-}$ cells expressing H-Ras^{L61} or H-Ras^{L61}-2A was not affected by overexpression of β-TrCP or Axin (Fig. 3E and fig. S7A). Moreover, the proliferation of *Gsk3*β$^{-/-}$ cells expressing oncogenic H-Ras^{L61} was higher than that of *Gsk3*β$^{+/+}$ cells expressing oncogenic H-Ras^{L61} (Fig. 3E and fig. S7A). The importance of the phosphorylation of oncogenic H-Ras in cellular transformation was also revealed by the loss of the inhibitory effects of β-TrCP and Axin on the anchorage-independent growth in cells expressing H-Ras^{L61}-2A (Fig. 3F and fig. S7B). Together, these results suggest that phosphorylation of H-Ras at Thr^{144} and Thr^{148} by GSK3β can inhibit cellular transformation caused by oncogenic H-Ras.

To confirm that GSK3β contributes to Ras destabilization in vivo, we inhibited GSK3β by administering LiCl to mice and then analyzed colon tissue for β-catenin and Ras abundance (Fig. 3G). Immunoblotting and immunohistochemical analyses showed that the abundance of β-catenin and Ras in colon tissue was increased in a dose-dependent manner by LiCl (Fig. 3G). Furthermore, intraperitoneal injection of ALLN to inhibit the proteasome resulted in the accumulation of both total Ras and p-Ras, and the abundance of p-Ras was reduced by LiCl (Fig. 3G).

Ras is stabilized in murine and human colon cancers

APC is another constituent of the β-catenin destruction complex, and mutations in the encoding gene are common causes of colon cancer (*26*). We found that overexpression of APC along with GSK3β enhanced H-Ras polyubiquitylation and increased the abundance of p-H-Ras and destabilized Myc-tagged H-Ras in HEK293 cells (fig. S8). We also identified an RKO

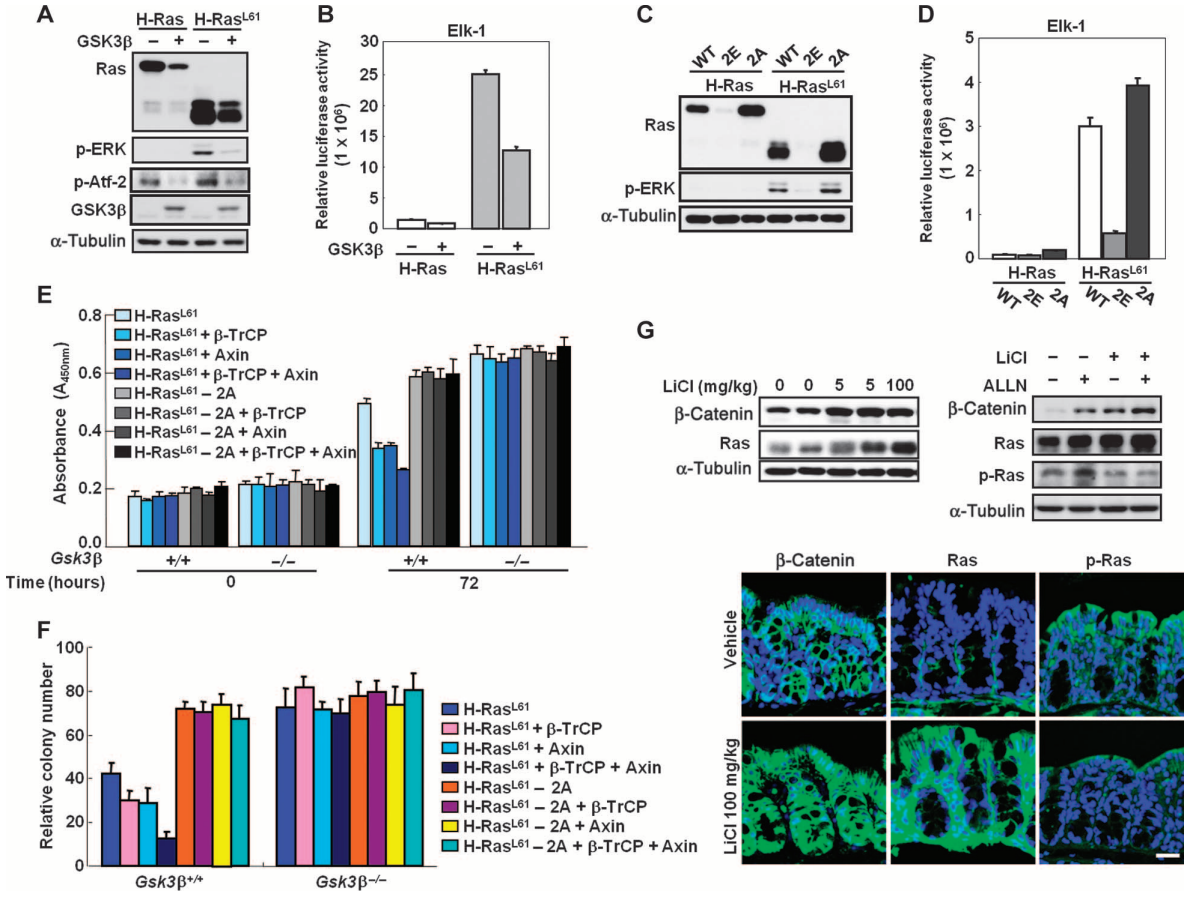

Fig. 3. Effects of the regulation of H-Ras stability on ERK pathway activation, cellular proliferation, and transformation. (**A**) Effect of GSK3β overexpression on H-Ras^{L61}–induced ERK pathway activity in HEK293 cells detected as phosphorylation of ERK and the ERK target Atf-2. (**B**) Effect of GSK3β overexpression on H-Ras^{L61}–induced ERK pathway activity in HEK293 cells detected as activity of an Elk-1 reporter construct. The relative luciferase activities were estimated by dividing individual luciferase activities by the value for β-gal. Values are given as means ± SD of three experiments. (**C**) Effects of H-Ras phosphorylation mutants on H-Ras^{L61}–induced ERK pathway activation in HEK293 cells detected as phosphorylation of ERKs. (**D**) Effects of H-Ras phosphorylation mutants on H-Ras^{L61}–induced ERK pathway activation in HEK293 cells detected as activity of an Elk-1 reporter construct and reported the same as for (B). (**E**) *Gsk3*β$^{+/+}$ and *Gsk3*β$^{-/-}$ cells were transfected with the indicated vectors, and cell proliferation was quantified at the indicated times after transfection. (**F**) *Gsk3*β$^{+/+}$ and *Gsk3*β$^{-/-}$ cells were transfected with the indicated vectors, and the number of colonies present after selection with G418 was calculated. Data are the average and SD of three experiments and presented as colony number relative to H-Ras^{L61}–expressing *Gsk3*β$^{+/+}$ cells. (**G**) Regulation of the stability of Ras by the GSK3 inhibitor LiCl and proteasomal inhibitor ALLN in mouse colon tissue. Top: Mice were injected with PBS or LiCl (100 mg/kg) (left) with or without DMSO or ALLN (38.3 mg/kg) 9 hours before tissue lysis (right). Whole-tissue lysates were subjected to immunoblot analyses. Bottom: Immunofluorescence staining was monitored by confocal microscopy. Scale bar, 20 μm.

Downloaded from stke.sciencemag.org on April 18, 2012

colorectal cancer cell retaining wild-type genes for the Wnt/β-catenin signaling components, and these cells exhibited increased abundance of both β-catenin and Ras proteins in response to Wnt3a stimulation (fig. S9).

To address the in vivo significance of the regulation of Ras stability by Wnt/β-catenin signaling, we adopted the well-established $Apc^{Min/+}$ and Apc^{1638N} murine models for intestinal tumorigenesis (*27*). We detected β-catenin and Ras staining at the plasma membrane of cells in the normal mucosa of the small intestine of wild-type mice. In contrast, we detected strong nuclear β-catenin staining in the adenomas of the small intestine of both $Apc^{Min/+}$ and Apc^{1638N} mice. Ras and ERK activation were also increased in the adenoma regions (Fig. 4A and fig. S10, A and B). Both β-catenin and Ras staining were increased in the adenocarcinomas of Apc^{1638N} mice (Fig. 4A). In contrast to the nuclear β-catenin, Ras in adenoma and adenocarcinoma was localized at the membrane and cytoplasm of cells. We also detected phosphorylated Atf-2 (p-Atf-2), indicating activation of the ERK pathway, in the adenomas of $Apc^{Min/+}$ and Apc^{1638N} mice (fig. S10, C and D). Consistent with the immunohistochemical results, immunoblot analysis showed an increase in β-catenin, Ras, and p-ERK in the tumors of $Apc^{Min/+}$ and Apc^{1638N} mice. Furthermore, p-Ras was decreased in adenomas compared to normal tissue (Fig. 4B).

We also examined Ras abundance in human colon specimens from familial adenomatous polyposis (FAP) patients (*28*). All FAP cases were determined on the basis of multiple polyp formation (>800) on the colonic mucosa (a representative gross image of FAP is shown in Fig. 4C, left bottom). The examined FAP patients included two cases each of adenoma and moderately differentiated adenocarcinoma. Nuclear β-catenin staining was strong in the tumor region, but not in the adjacent normal tissue (Fig. 4C). Consistent with the studies in mice, the abundance of Ras was increased in adenoma case 1 of a FAP patient in which nuclear β-catenin was increased (Fig. 4C). Similarly, in adenoma case 2, the staining pattern of Ras was correlated with the staining pattern of β-catenin, such that cells with a strong β-catenin signal also had a strong Ras signal (fig. S11A). ERK activity (p-ERK) was also increased in the tumor area where Ras was increased (Fig. 4C; see fig. S11B for validation of antibody specificity). However, higher magnification revealed differences in the intracellular localization of these proteins: Ras staining was observed in both the cytoplasm and the

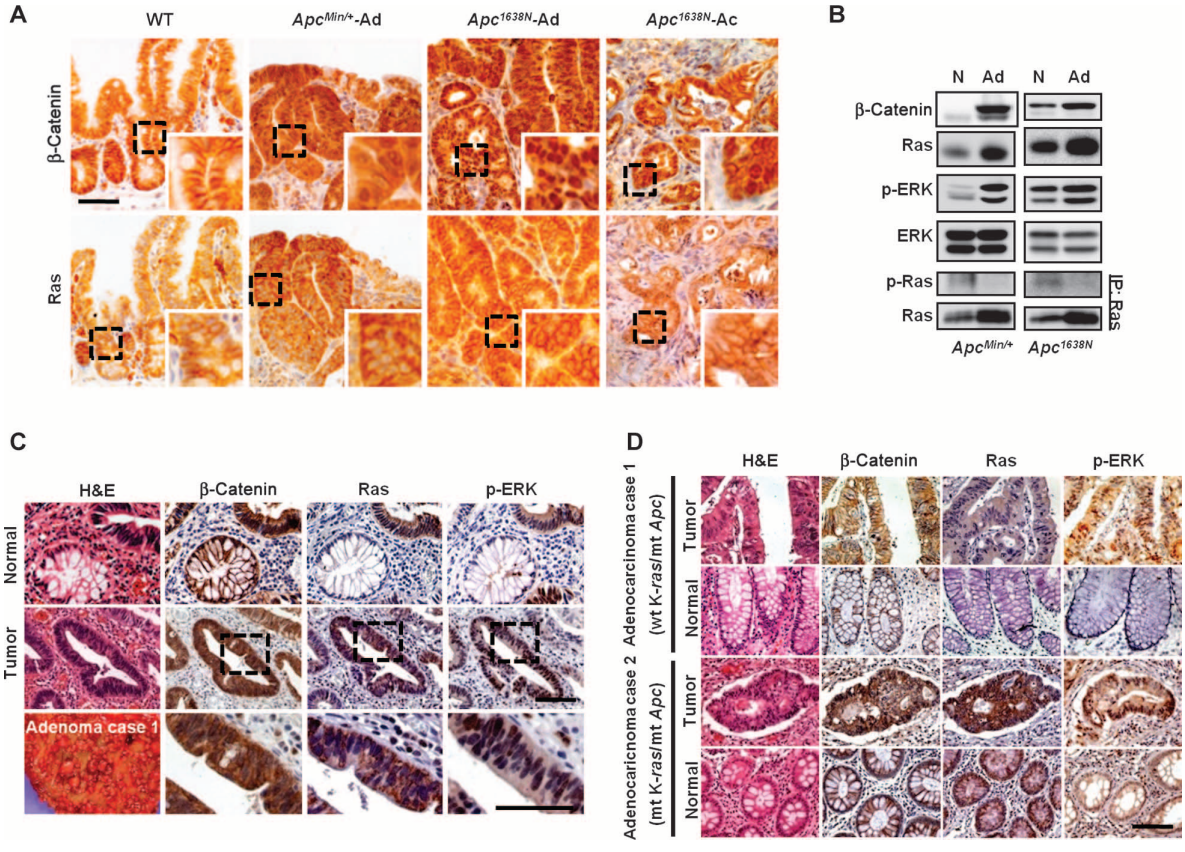

Fig. 4. Loss of *Apc* increases Ras abundance in murine colon and in human FAP colon samples. (**A**) Immunohistochemical analysis of β-catenin and Ras in adenomas and adenocarcinomas from $Apc^{Min/+}$ and Apc^{1638N} mice and normal mucosa of the small intestine from a WT mouse. Zoomed images (white solid box) are ×4 magnifications. Ad, adenoma; Ac, adenocarcinoma. (**B**) Immunoblot analyses of normal mucosa and adenoma tissues from $Apc^{Min/+}$ and Apc^{1638N} mice. WCLs were prepared and probed with antibodies recognizing the indicated proteins. For the bottom two sections, the extracts were immunoprecipitated with the anti-Ras antibody and probed with p-Ras or anti-Ras antibody. N, normal; Ad, adenoma. (**C** and **D**) Immunohistochemical analyses of adenoma (C) and adenocarcinoma (D) from FAP patients. Gross image of colon showing multiple polyps is labeled "Adenoma case 1" in (C). Histology of tumor and normal areas was analyzed by H&E staining, and β-catenin, Ras, and p-ERK were evaluated by immunohistochemical analyses. The bottom panels show higher-magnification images of the dotted box areas. All scale bars, 50 μm. See fig. S11D for details of the genotypes of the patient samples shown in adenocarcinoma case 1 and case 2.

Downloaded from stke.sciencemag.org on April 18, 2012

plasma membrane in the tumor area, whereas p-ERK staining was predominantly observed in the nucleus, and β-catenin was detected in the cytoplasm and nuclei of tumor cells (Fig. 4C, magnified images of the tumor regions are shown at the bottom). Immunoblot analysis of adenoma case 1 detected a truncated APC, indicative of FAP (fig. S11C), and also showed differences in β-catenin, Ras, and p-ERK from the normal tissue that were consistent with those observed by immunohistochemical analyses (Fig. 4C). Transcript analysis confirmed that the accumulation of Ras in tumor tissues was not mediated by the altered mRNA abundance (fig. S11C).

In the adenocarcinoma specimens, we identified *Apc* germline mutations of FAP patients with denaturing high-performance LC followed by sequencing analysis. A deletion mutation (c.3927_3931delAAAGA, p.Clu1309fsX4) was detected in adenocarcinoma case 1, whereas a nonsense mutation (c.1269G>A, p.Trp423X) was identified in adenocarcinoma case 2 (fig. S11D). Because K-*ras* mutations are known to occur after *Apc* mutations in colorectal tumorigenesis (*29*, *30*), we assessed the somatic mutational status of K-*ras* in all of the FAP patients at codons 12, 13, and 61. A point mutation at codon 12 was detected in adenocarcinoma case 2, whereas no mutations at codons 12, 13, or 61 were found in adenocarcinoma case 1 (fig. S11E). Increased Ras and β-catenin and increased ERK activity were observed in the tumors of both adenocarcinoma case 1 (wild-type K-*ras*) and case 2 (mutant K-*ras*) patients (*30*) (Fig. 4D). The overall staining patterns of β-catenin, Ras, and p-ERK in the FAP adenoma cases correlated, regardless of the mutational status of K-*ras*, indicating that Ras stabilization through aberrant Wnt/β-catenin signaling may contribute to colorectal tumorigenesis.

We also used a human tissue microarray (TMA) assay to investigate Ras abundance in normal and cancer tissues from different organs. The abundance of Ras was increased in many cancers including breast, lung, prostate, and lung cancers, but not in renal cell carcinoma (Fig. 5A). Because colon

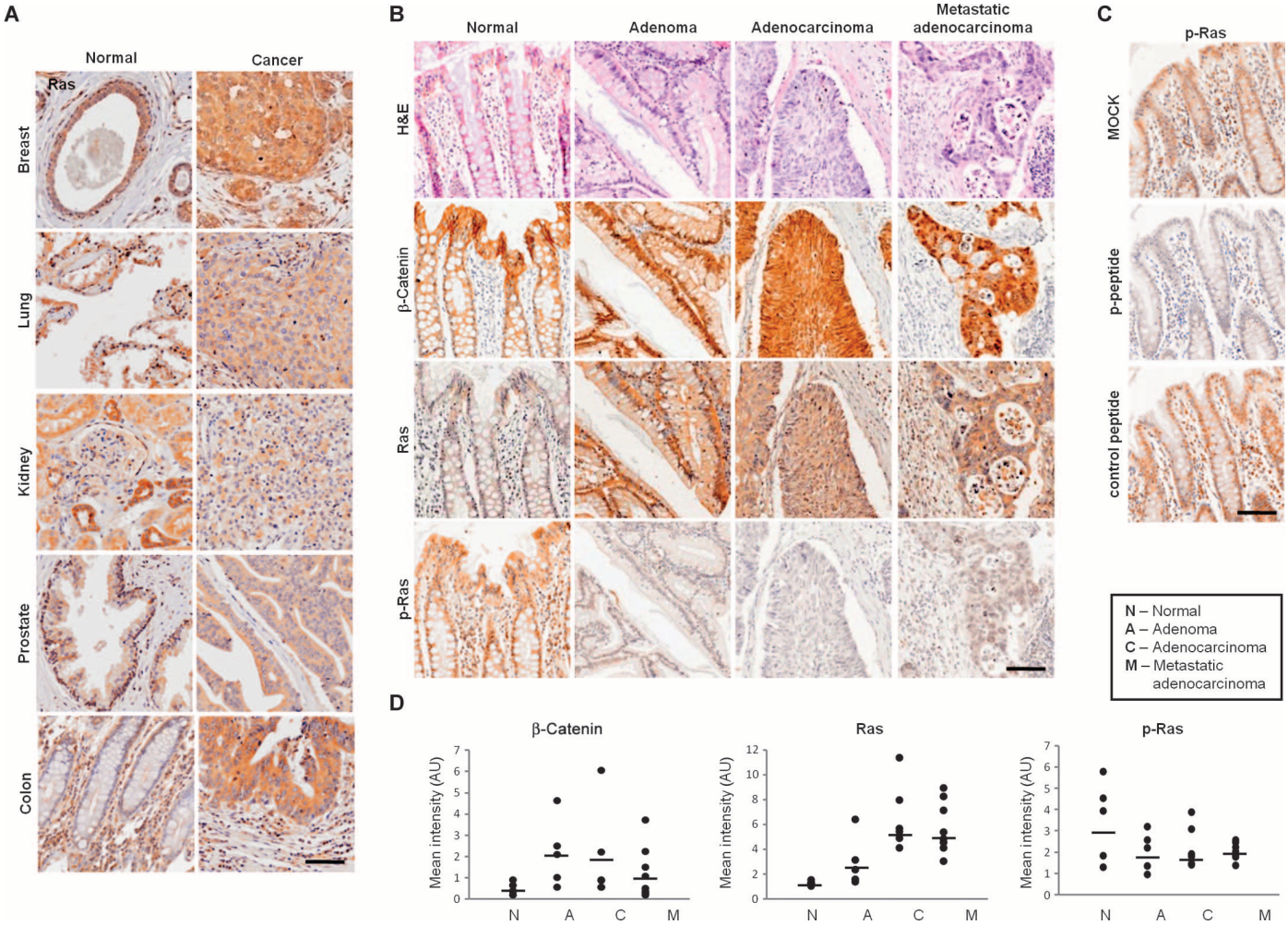

Fig. 5. The abundance of Ras is increased in various cancer tissues and in different stages of colon cancers. (**A**) Immunohistochemical analyses of Ras abundance in TMA samples of normal and cancerous regions of the indicated organs. Ras was detected with the anti-Ras antibody. (**B**) A representative example of immunohistochemical analyses for the indicated proteins of TMA containing normal, adenoma, adenocarcinoma, and metastatic adenocarcinoma colon specimens. (**C**) The specificity of p-Ras staining was confirmed by signal elimination by p-Ras peptide (p-peptide) but not by the control peptide. (**D**) Quantitative analysis was performed by comparing the mean intensity of the staining for β-catenin, Ras, or p-Ras among various stages of colon cancer. AU, arbitrary unit. All scale bars, 100 μm.

Downloaded from stke.sciencemag.org on April 18, 2012

cancer showed the greatest increase in Ras abundance, we examined the correlation between Ras, p-Ras, and β-catenin by human colon cancer TMA that included five normal, five adenoma, six adenocarcinoma, and eight metastatic adenocarcinoma cases (representative cases are shown in Fig. 5B). The abundance of Ras was high in adenoma and adenocarcinoma, as well as in metastatic adenocarcinoma, whereas weak Ras staining was observed in normal colon (Fig. 5B). Critically, strong Ras staining correlated with weak p-Ras staining, consistent with the role of phosphorylation in regulating Ras abundance. The specificity of the p-Ras signal in immunohistochemical analysis was confirmed by ablation of the signal by competition with the p-Ras peptide used for generation of p-Ras antibody and no effect of control peptide (Fig. 5C and fig. S12). Quantitative analyses showed an increase in Ras and a decrease in p-Ras during colon cancer progression in all cases (Fig. 5D). Overall, our data indicate that stabilization of Ras protein through its dephosphorylation correlated with the occurrence, progression, and metastasis of colon cancer.

DISCUSSION

Our studies showed that GSK3β, a negative regulator of the Wnt/β-catenin pathway, phosphorylates H-Ras at Thr^{144} and Thr^{148} within the TSAKT motif corresponding to the GSK3β consensus site S/TxxxS/T (*23*, *24*). This phosphorylation event recruited β-TrCP to Ras despite Ras lacking the conserved β-TrCP–binding motif (DpS/TGXXpS/T). This result indicates that either Ras retains a unique β-TrCP binding site or the phosphorylated motif in Ras represents a previously unknown β-TrCP binding site that may also be present in other phosphorylated proteins. Phosphorylation of Ras by GSK3β connects regulation of Ras stability to the Wnt/β-catenin signaling pathway; when Wnt signaling was inhibited by Axin or APC overexpression, we observed enhanced GSK3β binding to and phosphorylation of H-Ras. Our data indicated that β-TrCP mediated E3 ligase activity through the recognition of p-H-Ras, leading to H-Ras polyubiquitylation (Fig. 6). Furthermore, ERK pathway activity was reduced in cells overexpressing GSK3β and correlated with Ras stability. The importance of GSK3β and its phosphorylation of Ras in the reduction of oncogenic Ras activity and inhibition of oncogenic Ras–induced cellular proliferation and transformation was indicated by the lack of effect of Axin and β-TrCP overexpression in $Gsk3\beta^{-/-}$ cells or in cells expressing phosphorylation-deficient mutants within the oncogenic form of Ras ($H\text{-}Ras^{L61}$). Because cellular proliferation and transformation decreased concomitantly with the reduction in oncogenic Ras, which was mediated by the components of the β-catenin destruction complex, these results indicated that Wnt/β-catenin signaling may inhibit the degradation of the oncogenic form of Ras and thus promote the oncogenic activity of Ras. Moreover, cell proliferation and transformation induced by oncogenic Ras were greater in $Gsk3\beta^{-/-}$ than in $Gsk3\beta^{+/+}$ cells and correlated with the accumulation of Ras in $Gsk3\beta^{-/-}$ cells. Although GSK3β and β-TrCP were identified as major proteins involved in the destabilization of Ras, other mechanisms may contribute to Ras degradation because the abundance of Ras appeared reduced in the $Gsk3\beta^{-/-}$ cells overexpressing Axin.

The in vivo role of GSK3β in suppression of Ras-induced transformation was demonstrated in a previous study showing promotion of Ras-mediated cellular transformation in $Gsk3\beta^{-/-}$ MEFs and Ras-induced tumor formation in a corresponding xenograft model (*21*). We found that multiple components of the Wnt-regulated β-catenin destruction complex were involved in H-Ras degradation, including Axin, APC, and GSK3β. Furthermore, we found that addition of Wnt3a to inhibit the destruction complex reduced H-Ras polyubiquitylation and phosphorylation in cells, and in mouse models of colon cancer caused by inactive APC mutations, both β-catenin and Ras were more abundant in the cancerous tissue than in normal tissue, confirming the importance of the Wnt/β-catenin pathway in regulating Ras stability in vivo.

We also provided evidence for this Wnt/β-catenin–Ras connection in human colon cancer. TMA studies with various stages of human colon cancer tissues indicated that the phosphorylation and stability regulation of Ras plays an important role in pathogenesis in vivo. Compared with normal colon, tumors at every stage showed tight correlation between accumulation of β-catenin and Ras and a decrease in p-Ras. The regulation of Ras stability by Wnt/β-catenin signaling is particularly important because it provides a mechanistic basis for crosstalk between two major transforming signaling pathways. Potential crosstalk between the Wnt/β-catenin and the Ras-ERK pathways has been suggested in previous studies (*15*–*18*, *31*), but no mechanism has been defined. H-Ras mutation alone does not induce hepatocellular carcinoma (HCC), but a combination of genetic mutations

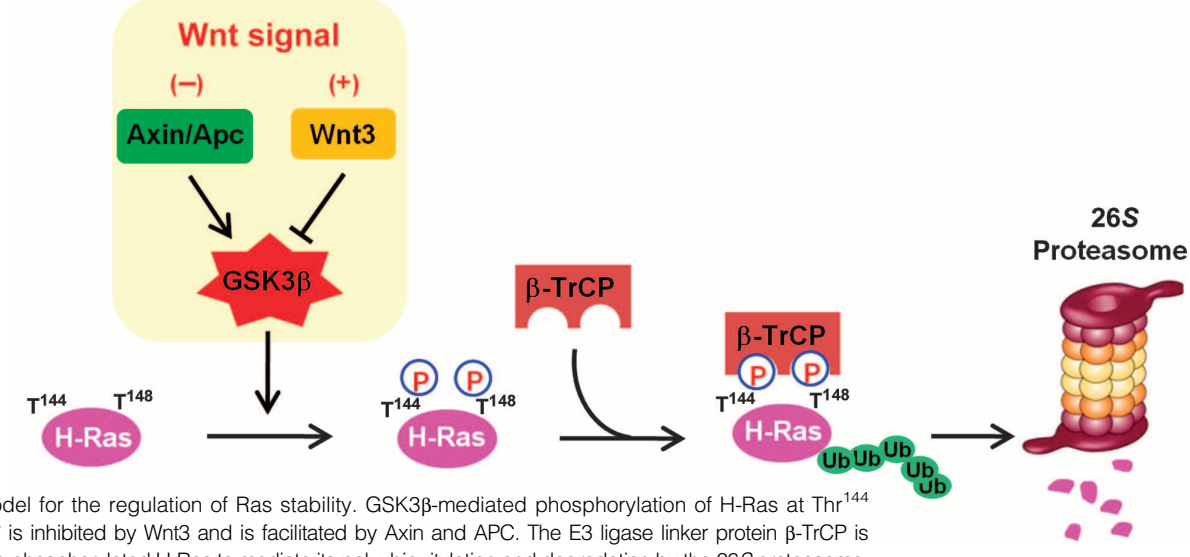

Fig. 6. Model for the regulation of Ras stability. GSK3β-mediated phosphorylation of H-Ras at Thr^{144} and Thr^{148} is inhibited by Wnt3 and is facilitated by Axin and APC. The E3 ligase linker protein β-TrCP is recruited to phosphorylated H-Ras to mediate its polyubiquitylation and degradation by the 26*S* proteasome.

Downloaded from stke.sciencemag.org on April 18, 2012

in H-Ras and β-catenin mutations results in a critical increase in the frequency of HCC in a mouse model (*16*). Stabilization of Ras through Wnt/β-catenin signaling also provides a potential molecular mechanism to explain previous observations of a genetic interaction between the genes encoding proteins in the Wnt/β-catenin pathway and *Ras* in the tumorigenesis of several different types of cancer in mice (*15*, *17*, *18*, *31*). The Ras accumulation in human colorectal cancers may be caused by DNA amplification or transcriptional activation. The amplification of DNA was observed in several cancers including colorectal cancers (*32*, *33*). However, the copy number information for the genes encoding K-Ras or N-Ras in the Oncomine database (http://www.oncomine.org) did not significantly change in colorectal cancers compared with paired normal samples (fig. S13). The mRNA abundances for K-, N-, and H-Ras were not significantly different between adenoma and normal epithelium (fig. S14). Therefore, the DNA amplification and transcriptional activation may not be a major cause for the Ras contribution to human colorectal cancer patients. Currently, regulation of the ERK pathway by *Apc* mutation is controversial. Different studies have reported either decreased ERK activity in human colorectal tumors (*31*) or increased ERK activity in adenoma of $Apc^{Min/+}$ mice (*34*) compared with adjacent normal tissue. The ERK activation pattern in mice with *Apc* loss varies depending on the size of tumors (*35*). The different results for ERK pathway activation in the context of *Apc* deficiency are not clear, but the stage or size of the tumor or tissue context could contribute to ERK activation status. We observed similar local activation of ERK in the small tumors or in the border area of large tumors from $Apc^{Min/+}$ mice without gross activation of ERK throughout the tumor (fig. S10B). Transient and short-term ERK activation may be sufficient for cancer cell proliferation, and ERK activity is tightly regulated by feedback regulation loops even in cancer (*36*, *37*).

In summary, we present a previously unknown mechanism for the destabilization of Ras that involves GSK3β-mediated phosphorylation of Ras and that is inhibited by Wnt/β-catenin signaling. This stabilization of Ras by Wnt/β-catenin signaling stimulates downstream ERK signaling and cellular proliferation and ultimately leads to tumor development. Additionally, we provide in vivo evidence for a role of this Ras stabilization pathway in colorectal tumorigenesis. However, further investigation with large numbers of human specimen need to be performed to provide more convincing data for the Ras stabilization related with pathophysiology. The destabilization of Ras proteins by the β-catenin destruction complex represents an attractive target for the development of Ras-regulating drugs and provides useful information for designing and evaluating clinical interventions for the management of human cancers caused by aberrant activation of the Wnt/β-catenin and Ras-ERK pathways.

MATERIALS AND METHODS

Cell culture, transfection, and drug treatment

HEK293 cells were maintained in Dulbecco's modified Eagle's medium (DMEM) (Gibco) supplemented with 10% fetal bovine serum (FBS). Immortalized $Gsk3\beta^{+/+}$ and $Gsk3\beta^{-/-}$ MEF cells were provided by J. Woodgett (Mount Sinai Hospital–Samuel Lunenfeld Research Institute, Toronto, Canada) and cultured as previously described (*38*). RKO cells were maintained in RPMI 1640 (Gibco) containing 10% FBS. Plasmid transfections were performed with Lipofectamine (Invitrogen) according to the manufacturer's instructions. The following drugs and recombinant proteins were administered at the indicated concentrations: ALLN (25 μg/ml), CHX (50 μg/ml), EGF (20 ng/ml), LiCl (20 mM), and Wnt3a (100 ng/ml). Recombinant Wnt3a protein was purchased from R&D Systems. All other chemicals were purchased from Sigma-Aldrich.

Plasmids and siRNA

The following constructs have been described previously (*8*, *19*, *20*): pcDNA3.1–H-Ras, pMT3–H-Ras^{L61}, pcDNA3.1–Flag–β-TrCP, pCS2-MT-Axin, pSUPER-Axin siRNA, pCMV-APC, pFA2–Elk-1, pFR-Luc reporter plasmid, pCMV–β-galactosidase (β-gal) reporter, pCS4-3xHA-Ub, and pCS4-3xFlag-Ub. p-RSET–His–H-Ras was provided by M. A. White (University of Texas Southwestern Medical Center, Dallas, TX) (*39*), and pDEST40-Axin1 and pDEST40-$Axin^{\Delta Ex4-5}$ were provided by R. C. Sears (Oregon Health and Science University, Portland, OR) (*22*). The pcDNA3.1-GSK3β-V5 and pcDNA3.1-GSK3β-K85M-V5 plasmids were a gift from T. Hagen (University Hospital, Nottingham, UK). The pEGFP-C3–H-Ras, pEGFP-C3–K-Ras, and pEGFP-C3–N-Ras constructs were provided by Y. I. Henis (Tel Aviv University, Israel) (*40*). Full-length K- and N-Ras sequences were isolated from an HEK293 cell complementary DNA (cDNA) library by polymerase chain reaction (PCR). For K-Ras, the following primers were used: (forward) 5′-CGGGATCCATGACTGAATATAAACTTGTG-3′ and (reverse) 5′-CGGGGTACCCATAATTACACACTTTGTCTT-3′. These primers included 5′ Kpn I and 3′ Bam HI restriction sites, which were used for insertion of the products into the pcDNA3.1-myc vector (Invitrogen). For N-Ras, the following primers were used: (forward) 5′-CGGAATTCATGACTGAGTACAAACTGGTG-3′ and (reverse) 5′-CCCAAGCTTCATCACCACACATGGCAATCC-3′. These primers included 5′ Eco RI and 3′ Hind III restriction sites, which were used for insertion of the products into the pcDNA3.1-myc vector. The H-, K-, and N-Ras mutants containing deletion of the HVR (H-, K-, and N-Ras–ΔHVR), mutations of the H-Ras phosphorylation sites, and pcDNA3-GSK3βS9A-HA were generated by PCR-based mutagenesis (Stratagene). All constructs and mutations were confirmed by nucleotide sequencing analyses. The siRNA sequences for Axin were described previously (*20*). The siRNA sequences for GSK3β (NM_002093) were 5′-CACUGAUUAUACCUCUAGU-3′ and 5′-CACUGUAACAUAGUCCGAU-3′. The green fluorescent protein (GFP) siRNA used for the negative control was 5′-GUUCAGCGUGUCCGGCGAGTT-3′ (synthesized by Bioneer).

Immunoprecipitation, in vivo ubiquitination assay, and immunoblotting

Immunoprecipitation and in vivo ubiquitination assays were performed as previously described (*8*). Briefly, cells were washed in ice-cold phosphate-buffered saline (PBS; Gibco) and lysed with radioimmunoprecipitation assay (RIPA) buffer (Upstate Biotechnology). Ten millimolar *N*-ethylmaleimide (NEM; Sigma-Aldrich) was subsequently added to the RIPA buffer for the in vivo ubiquitination assays. The lysates were incubated with the indicated antibodies and protein A/G agarose at 4°C for 12 hours, and the immunoprecipitated beads were washed three times in RIPA buffer. In vivo ubiquitination assays were performed under denaturing conditions when necessary. Denatured cell extracts were prepared by resuspending cell pellets in 1 ml of denaturing buffer [50 mM tris (pH 7.5), 150 mM NaCl, 1% SDS, and 10 mM NEM] and boiled for 10 min. Immunoprecipitation assays were performed with an antibody recognizing Myc after addition of 9 ml of tris-buffered saline (TBS) buffer [50 mM tris (pH 7.5) and 150 mM NaCl] together with 0.5% NP-40 and 10 mM NEM. The immune complexes were resolved by SDS–polyacrylamide gel electrophoresis (SDS-PAGE), and immunoblotting was performed as previously described (*8*). Antibodies were obtained from the following sources: anti-GSK3β, anti-Myc, anti–p-Atf-2, and anti–p-ERK from Cell Signaling Technology; anti-HA (hemagglutinin), anti-GST (glutathione *S*-transferase), anti-APC (C-20), and anti–β-catenin from Santa Cruz Biotechnology; anti-Ras (clone Ras10) and anti-Axin from Upstate Biotechnology; anti–α-tubulin from Calbiochem; anti–H-Ras from Oncogene Research Products; anti–β-TrCP

Downloaded from stke.sciencemag.org on April 18, 2012

from Zymed; anti-V5 from Invitrogen; and anti-Flag from Sigma-Aldrich. Phospho-T^{144}/T^{148} H-Ras polyclonal antibodies were generated by immunizing rabbits with a keyhole limpet hemocyanin (KLH) carrier protein–conjugated phosphorylated peptide (residues 140 to 152; PYIEpTSAKpTRQGV; Abmart Inc.). Secondary antibodies were horseradish peroxidase (HRP)–conjugated anti-mouse (Cell Signaling Technology) and anti-rabbit (Bio-Rad).

Identification of H-Ras phosphorylation sites

A 40-μl sample of His–H-Ras phosphorylated by GSK3β was separated by 10% SDS-PAGE, and the H-Ras protein bands were excised for in-gel digestion with trypsin (25 ng/ml; Promega). The enrichment of phosphopeptides from tryptic digests was performed with TiO_2 microcolumns as previously described (*41*). The phosphopeptides were analyzed by nano-electrospray LC-MS/MS. High-pressure LC separation was performed on an Ultimate instrument equipped with a Famos Autosampler (LC Packings) at a flow rate of 200 nl/min. The columns were constructed from fused silica capillary tubes (360-μm outer diameter and 75-μm inner diameter) and packed with 300 Å C18 beads (5-μm diameter; Grace Vydac) to a length of 15 cm. The MS/MS were recorded on an API QSTAR Pulsar Q-TOF (quadrupole orthogonal acceleration–time-of-flight) mass spectrometer (Applied Biosystems) in the information-dependent acquisition mode. The MS/MS spectra were used to search the National Center for Biotechnology Information (NCBI) nonredundant and expressed sequence tag databases with the computer algorithm Mascot or proID (Applied Biosystems).

Preparation of recombinant proteins

For kinase assays, recombinant proteins were purified from *Escherichia coli* C41 transformed with p-RSET-A–His–H-Ras or p-RSET-A–His–H-Ras-T144/T148A (His–H-Ras-2A) and induced with 0.25 mM isopropyl-β-D-thiogalactopyranoside (IPTG). His–H-Ras or His–H-Ras-2A extracts were prepared by sonication in buffer [25 mM tris (pH.8.0), 100 mM NaCl, and 30 mM imidazole]. The *E. coli* extracts were applied to Ni-NTA (nitrilotriacetic acid)–Sepharose resin (Qiagen), and His–H-Ras or His–H-Ras-2A was eluted with elution buffer [25 mM tris (pH.8.0), 100 mM NaCl, and 500 mM imidazole]. Eluted proteins were dialyzed with kinase buffer with a 3500 molecular weight cutoff membrane.

In vitro kinase assay

In vitro kinase analyses were performed with 2 μg of purified His–H-Ras and 200 ng of recombinant human active GSK3β (R&D Systems) in 20 μl of kinase buffer [50 mM tris-HCl (pH 7.5), 10 mM $MgCl_2$, and 1 mM dithiothreitol (DTT)] containing 10 mM adenosine 5′-triphosphate (ATP) and 10 μCi [γ-^{32}P]ATP (PerkinElmer Life Sciences) for 4 hours at 30°C. Reactions were stopped by addition of 5× SDS sample buffer and heating at 95°C. The samples were separated by 10% SDS-PAGE, and images were obtained by autoradiography of the dried gels.

Immunocomplex kinase assay

Cells were transfected with pcDNA3-GSK3βS9A-HA or pcDNA3-GSK3βK85M-HA for 48 hours and lysed with RIPA buffer, and solubilized fractions were subjected to immunoprecipitation with anti-HA antibody to precipitate HA-GSK3β. Immunocomplex kinase assays were performed by incubating the immunopellets for 2 hours at 30°C with 2 μg of His–H-Ras or His–H-Ras-2A recombinant protein in 20 μl of kinase buffer containing 10 mM ATP and 10 μCi [γ-^{32}P]ATP. The reaction was terminated by addition of 5× SDS sample buffer and heating at 95°C. The reaction mixture was subjected to SDS-PAGE on a 12% polyacrylamide gel, and images were obtained by autoradiography of the dried gels.

In vitro ubiquitination assay

For the in vitro ubiquitination assay, purified H-Ras was phosphorylated by GSK3β and then incubated in a reaction buffer containing 25 mM tris-HCl (pH 7.5), 50 mM NaCl, 5 mM ATP, 10 mM $MgCl_2$, 1 mM DTT, 1 μg of ubiquitin, 250 ng of Uba1, 500 ng of UbcH5a, and $SCF^{β\text{-}TrCP}$ complex. For the preparation of $SCF^{β\text{-}TrCP}$ complex proteins, Uba, Cul1, and RBX1 were isolated from transfected HeLa cells, and β-TrCP was purified from transfected 293T cells with Flag resin (Sigma). UbcH5a was purified from *E. coli*. SKP1 and ubiquitin were purchased from ATGen or Enzo Biochem Inc. After incubation at 25°C for 4 hours, the reaction was terminated by the addition of SDS sample buffer and analyzed by Western blotting analysis with an anti-Ras (clone Ras10) antibody.

Elk-1 reporter assay

Cells were transfected with the indicated combinations of the following plasmids: pcDNA3.1–H-Ras, -2E, or -2A; pMT3–H-Ras^{L61}, -2E, -2A; pcDNA3.1-GSK3β-V5, together with pFA2–Elk-1, pFR-Luc plasmid, and pCMV–β-gal reporter (Clontech). At 24 hours after transfection, the cells were treated with 20 ng of EGF for 12 hours as required. Cells were harvested and lysed in the reporter lysis buffer according to the manufacturer's instructions (Promega). Luciferase activities were normalized to β-gal levels as an internal control. The results are expressed as the means ± SD from three independent experiments.

Cell proliferation assay

Plasmid transfections were performed as indicated in *Gsk3*$β^{+/+}$ or *Gsk3*$β^{-/-}$ cells, which were subsequently seeded into 96-well plates. Viable cell numbers were determined at 0, 24, 48, and 72 hours after seeding by a colorimetric assay with a Cell Counting Kit-8 proliferation assay kit (Dojindo Laboratories). The absorbance at 420 nm was monitored with a Fluostar Optima microplate reader (BMG Labtech). The results are expressed as the means ± SD from three independent experiments.

Animals and tissue preparation

Mice were maintained according to standard protocols and fed a standard maintenance diet from Dae Han Bio Link. C57BL/6J-*Apc*$^{Min/+}$ and C57BL/6J-*Apc*^{1638N} mice were obtained from Jackson Laboratory and National Cancer Institute mouse repository, respectively. Mice were housed in microventilation cage system (MVCS) cages with a computerized environmental control system (Threeshine Inc.). Room temperature was maintained at 24°C with a relative humidity of 40 to 70%. For tissue preparation, intestinal and colon tissues from the mice were removed immediately after mice were killed. The abdomens of the mice were cut open longitudinally and cleaned by flushing with PBS. Tumor tissues and enterocytes from *Apc*$^{Min/+}$ or *Apc*^{1638N} mice were obtained as previously described (*42*). To investigate the in vivo regulation of Ras stability by Wnt/β-catenin signaling, we intravenously injected PBS or LiCl into the tail vein of 12-week-old male ICR mice (5 or 100 mg/ml) daily for 7 days. Dimethyl sulfoxide (DMSO) or ALLN (38.3 mg/ml) was injected intraperitoneally 9 hours before mice were killed. The animal studies were approved and performed under the guidelines of the Institute of Health Guidelines for the Institutional Review Board of Severance Hospital, Yonsei University College of Medicine (Seoul, Korea).

Immunohistochemistry

Paraformaldehyde-fixed paraffin sections were deparaffinized and rehydrated. For antigen retrieval, the slides were autoclaved in 10 mM sodium citrate buffer. Sections were preincubated in PBS and then blocked in 5% bovine serum albumin (BSA) and 1% goat serum in PBS at room temperature for 30 min. The sections were incubated with primary antibody

Downloaded from stke.sciencemag.org on April 18, 2012

overnight at 4°C. Antibodies recognizing proliferating cell nuclear antigen (PCNA) or 5-bromo-2′-deoxyuridine (BrdU) were purchased from Santa Cruz Biotechnology and Dako, respectively. Antibodies recognizing p-ERK (IHC Preferred) or p-Atf-2 (T^{71}) were purchased from Cell Signaling Biotechnology. The antibodies recognizing Ras or β-catenin were obtained from Millipore and BD Biosciences, respectively. The concentrations of the primary antibodies were as follows: PCNA (1:500), BrdU (1:200), β-catenin (1:200), p-ERK (1:20 to 1:100), p-Atf-2 (1:50), and Ras (1:100). For immunofluorescence staining, the sections were then incubated with Alexa Fluor 488– or Alexa Fluor 555–conjugated immunoglobulin G secondary antibody (Molecular Probes; 1:500) at room temperature for 1 hour, counterstained with 4′,6-diamidino-2-phenylindole (DAPI) (Boehringer Mannheim), and mounted in Gel/Mount medium. Visualization of fluorescence signal was performed by confocal microscopy (LSM510, Carl Zeiss) at excitation wavelengths of 488 nm (Alexa Fluor 488), 543 nm (Alexa Fluor 555), and 405 nm (DAPI). All incubations were carried out in the dark in humid chambers. For diaminobenzidine (DAB) staining, immunohistochemistry was performed with the UltraTek HRP kit (Scytek Laboratories Inc.). The DAB-stained preparations were visualized with a general optical microscope (Nikon TE-200U). The primary antibody was omitted for negative control slides, resulting in very low background labeling. The specificity of p-ERK staining was confirmed by specific inhibition of p-ERK staining after co-incubation with a p-ERK–specific blocking peptide (Santa Cruz Biotechnology). At least four fields per section were analyzed to establish reproducibility.

Patients and TMA

Four unrelated FAP patients were analyzed in this study. All cases were identified in the Department of Pathology at Yonsei University Medical Center between 2003 and 2005 for molecular marker studies. The fresh specimens were stored and obtained from the Cancer Specimen Bank of the National Research Resource Bank Program of the Korea Science and Engineering Foundation of the Ministry of Science and Technology. Authorization to use these tissues for research purposes was obtained from the Institutional Review Board of Yonsei Medical Center. The differentiation grades of the tumors were evaluated according to the guidelines of the American Joint Commission on Cancer. All FAP colons had >800 polyps. The tissue specimens were fixed in 10% neutral-buffered formalin, dehydrated by serial immersion in alcohol, cleared in xylene, and embedded in paraffin. For histological analyses, 4-μm-thick sections were cut from tissue blocks with an RM2245 microtome from Leica Microsystems. For protein extraction, fresh tumor tissues were obtained immediately after surgical excision for available cases and stored at −80°C before use. TMAs for normal and cancer tissues from various organs (BC8) and colon disease spectrum (BC05002) were purchased from SuperBioChips and US Biomax, respectively. Immunohistochemistry was performed with antibodies against β-catenin, Ras, or p-Ras. The specificity of the p-Ras antibody was confirmed by a competition experiment with phosphospecific and control peptides. The TMA slides were scanned with the BX51 virtual microscopy system (Olympus) at 40× objective magnification. For quantitative analysis, the intensity of each staining was determined by HistoFAX software (TissueGnostics).

Anchorage-independent growth assay

Anchorage-independent cell growth was monitored by assaying the colony-forming ability of cells in soft agar as previously described (*20*). Briefly, *Gsk3*$\beta^{+/+}$ or *Gsk3*$\beta^{-/-}$ cells were transiently transfected with the combinations of plasmids indicated and cultured in 10% FBS–DMEM for 2 days. Cells were mixed with equal volumes of 1.2% agar solution and 2× DMEM/20% FBS and then immediately transferred to the wells of a 96-well flat-bottom microplate containing an identical solidified base agar layer. Medium was added on top of the agar and changed once per week to compensate for evaporation, and colonies were scored after 20 days. The results are expressed as the means ± SD from three independent experiments.

Mutational analysis of *Apc*

For mutational analyses of *Apc* genes in FAP patient specimens, peripheral blood lymphocytes were isolated from patient blood samples and the *Apc* gene was amplified by PCR. To analyze the mutational status of the *Apc* gene, we performed denaturing high-performance liquid chromatography (DHPLC) analysis through all the coding exons of the *Apc* gene. All samples showing abnormal patterns in the DHPLC analysis were subjected to DNA sequencing analysis.

DHPLC analysis

DHPLC was performed with a WAVE MD DNA fragment analysis system with a DNASep column (Transgenomic Inc.). DNASep columns contain nonporous alkylated polystyrene-divinylbenzene particles that are both electrically neutral and hydrophobic; thus, the negatively charged phosphate ions of DNA molecules cannot bind to the column unaided. Triethylammonium acetate (TEAA) is a positively charged reagent that facilitates the interaction between the stationary matrix and the DNA molecules. DNA fragments are eluted from the column by reducing the hydrophobic interaction between the alkyl chains of TEAA and the stationary phase of the column. This is achieved by altering the ratio of TEAA to acetonitrile. The DNA molecules eluted from the column are detected by scanning with an ultraviolet C detector. The successful resolution of heteroduplexes from homoduplexes requires an elution gradient at a partially denaturing temperature. At this temperature, only heteroduplexes are destabilized by the mismatched bases, such that they are slightly more melted than the homoduplexes, resulting in earlier elution than the homoduplexes. This special resolution temperature was predicted by use of DHPLC Melt software (http://insertion.stanford.edu/melt.html). After denaturation, reannealed PCR products were injected onto the column and eluted with a linear acetonitrile gradient at a flow rate of 0.9 ml/min, with a mobile phase consisting of a mixture of buffers A (0.1 M TEAA and 1 mM EDTA) and B (25% acetonitrile in 0.1 M TEAA).

Mutational analysis of *K-ras*

Total genomic DNA was extracted from hematoxylin and eosin (H&E)–stained paraffin sections of 10-μm thickness containing a representative portion of each colorectal tumor block by means of the QIAamp DNA Mini Kit (Qiagen). Fifty nanograms of DNA was amplified in a 20-μl reaction solution containing 2 μl of 10× buffer (Roche), $MgCl_2$ (1.7 to 2.5 mM), 0.3 μM each primer pair [codons 12 and 13: (forward) 5′-TTATGTGTGACATGTTCTAAT-3′, (reverse) 5′-AGAATGGTCCTGCACCAGTAA-3′; codon 61: (forward) 5′-TCAAGTCCTTTGCCCATTTT-3′, (reverse) 5′-TGCATGGCATTAGCAAAGAC-3′], 250 μM deoxynucleotide triphosphates, and 2.5 U DNA polymerase (Roche). Amplification was performed with a 5-min initial denaturation at 94°C followed by 30 cycles of 1 min at 94°C, 1 min at 55°C, and 1 min at 72°C, and a 10-min final extension at 72°C. PCR products were separated on a 2% agarose gel and gel-purified with a QIAgen gel extraction kit (Qiagen) before being subjected to DNA sequencing analysis.

SUPPLEMENTARY MATERIALS

www.sciencesignaling.org/cgi/content/full/5/219/ra30/DC1

Fig. S1. Role of GSK3β and Axin in the regulation of H-Ras stability.

Fig. S2. H-Ras phosphorylation at Ser^{183} is not involved in its degradation.

Fig. S3. The role of β-TrCP in regulating the stability of K- and N-Ras.

Downloaded from stke.sciencemag.org on April 18, 2012

Fig. S4. Thr^{144} and Thr^{148} of H-Ras are phosphorylated by GSK3β and are involved in its degradation.
Fig. S5. Effects of H-Ras stabilization through GSK3β-mediated phosphorylation on ERK pathway activation by EGF.
Fig. S6. Subcellular localization of Ras and p-Ras.
Fig. S7. GSK3β inhibits cellular proliferation and transformation induced by oncogenic Ras through phosphorylation and subsequent degradation of H-Ras.
Fig. S8. Effects of APC upon degradation and polyubiquitylation of H-Ras by overexpression of GSK3β.
Fig. S9. Effects of Wnt3a on the stability of β-catenin and Ras in RKO cells.
Fig. S10. Immunohistochemical analyses of $Apc^{Min/+}$ and Apc^{1638N} mice.
Fig. S11. Immunohistochemical and immunoblot analyses and mutational status of *Apc* and *K-Ras* genes of adenocarcinoma from FAP patients.
Fig. S12. Specificity test for the antibody that detects phosphorylated Ras in immunohistochemical analyses.
Fig. S13. DNA copy numbers of *K-Ras*, *N-Ras*, *TOP1*, and *GAPDH* in human colorectal adenocarcinoma.
Fig. S14. mRNA expression of *K-*, *N-*, and *H-Ras* and *PCNA* in human colorectal adenoma.

REFERENCES AND NOTES

1. P. A. Konstantinopoulos, M. V. Karamouzis, A. G. Papavassiliou, Post-translational modifications and regulation of the RAS superfamily of GTPases as anticancer targets. *Nat. Rev. Drug Discov.* **6**, 541–555 (2007).
2. J. L. Bos, *ras* oncogenes in human cancer: A review. *Cancer Res.* **49**, 4682–4689 (1989).
3. Y. Pylayeva-Gupta, E. Grabocka, D. Bar-Sagi, RAS oncogenes: Weaving a tumorigenic web. *Nat. Rev. Cancer* **11**, 761–774 (2011).
4. I. R. Vetter, A. Wittinghofer, The guanine nucleotide–binding switch in three dimensions. *Science* **294**, 1299–1304 (2001).
5. S. Schubbert, K. Shannon, G. Bollag, Hyperactive Ras in developmental disorders and cancer. *Nat. Rev. Cancer* **7**, 295–308 (2007).
6. N. Jura, E. Scotto-Lavino, A. Sobczyk, D. Bar-Sagi, Differential modification of Ras proteins by ubiquitination. *Mol. Cell* **21**, 679–687 (2006).
7. A. Lorentzen, A. Kinkhabwala, O. Rocks, N. Vartak, P. I. Bastiaens, Regulation of Ras localization by acylation enables a mode of intracellular signal propagation. *Sci. Signal.* **3**, ra68 (2010).
8. S. E. Kim, J. Y. Yoon, W. J. Jeong, S. H. Jeon, Y. Park, J. B. Yoon, Y. N. Park, H. Kim, K. Y. Choi, H-Ras is degraded by Wnt/β-catenin signaling via β-TrCP-mediated polyubiquitylation. *J. Cell Sci.* **122**, 842–848 (2009).
9. B. Zhang, A. Ougolkov, K. Yamashita, Y. Takahashi, M. Mai, T. Minamoto, β-*Catenin* and *ras* oncogenes detect most human colorectal cancer. *Clin. Cancer Res.* **9**, 3073–3079 (2003).
10. H. Clevers, Wnt/β-catenin signaling in development and disease. *Cell* **127**, 469–480 (2006).
11. C. Liu, Y. Kato, Z. Zhang, V. M. Do, B. A. Yankner, X. He, β-Trcp couples β-catenin phosphorylation-degradation and regulates *Xenopus* axis formation. *Proc. Natl. Acad. Sci. U.S.A.* **96**, 6273–6278 (1999).
12. A. Salic, E. Lee, L. Mayer, M. W. Kirschner, Control of β-catenin stability: Reconstitution of the cytoplasmic steps of the Wnt pathway in *Xenopus* egg extracts. *Mol. Cell* **5**, 523–532 (2000).
13. V. Korinek, N. Barker, P. J. Morin, D. van Wichen, R. de Weger, K. W. Kinzler, B. Vogelstein, H. Clevers, Constitutive transcriptional activation by a β-catenin–Tcf complex in $APC^{-/-}$ colon carcinoma. *Science* **275**, 1784–1787 (1997).
14. P. J. Morin, A. B. Sparks, V. Korinek, N. Barker, H. Clevers, B. Vogelstein, K. W. Kinzler, Activation of β-catenin–Tcf signaling in colon cancer by mutations in β-catenin or APC. *Science* **275**, 1787–1790 (1997).
15. G. M. D'Abaco, R. H. Whitehead, A. W. Burgess, Synergy between Apc^{min} and an activated *ras* mutation is sufficient to induce colon carcinomas. *Mol. Cell. Biol.* **16**, 884–891 (1996).
16. N. Harada, H. Oshima, M. Katoh, Y. Tamai, M. Oshima, M. M. Taketo, Hepatocarcinogenesis in mice with β-catenin and Ha-ras gene mutations. *Cancer Res.* **64**, 48–54 (2004).
17. K. P. Janssen, P. Alberici, H. Fsihi, C. Gaspar, C. Breukel, P. Franken, C. Rosty, M. Abal, F. El Marjou, R. Smits, D. Louvard, R. Fodde, S. Robine, *APC* and oncogenic *KRAS* are synergistic in enhancing Wnt signaling in intestinal tumor formation and progression. *Gastroenterology* **131**, 1096–1109 (2006).
18. H. B. Pearson, T. J. Phesse, A. R. Clarke, K-ras and Wnt signaling synergize to accelerate prostate tumorigenesis in the mouse. *Cancer Res.* **69**, 94–101 (2009).
19. K. S. Park, S. H. Jeon, S. E. Kim, Y. Y. Bahk, S. L. Holmen, B. O. Williams, K. C. Chung, Y. J. Surh, K. Y. Choi, APC inhibits ERK pathway activation and cellular proliferation induced by RAS. *J. Cell Sci.* **119**, 819–827 (2006).
20. S. H. Jeon, J. Y. Yoon, Y. N. Park, W. J. Jeong, S. Kim, E. H. Jho, Y. J. Surh, K. Y. Choi, Axin inhibits extracellular signal-regulated kinase pathway by Ras degradation via β-catenin. *J. Biol. Chem.* **282**, 14482–14492 (2007).
21. S. Liu, X. Fang, H. Hall, S. Yu, D. Smith, Z. Lu, D. Fang, J. Liu, L. C. Stephens, J. R. Woodgett, G. B. Mills, Homozygous deletion of glycogen synthase kinase 3β bypasses senescence allowing Ras transformation of primary murine fibroblasts. *Proc. Natl. Acad. Sci. U.S.A.* **105**, 5248–5253 (2008).
22. H. K. Arnold, X. Zhang, C. J. Daniel, D. Tibbitts, J. Escamilla-Powers, A. Farrell, S. Tokarz, C. Morgan, R. C. Sears, The Axin1 scaffold protein promotes formation of a degradation complex for c-Myc. *EMBO J.* **28**, 500–512 (2009).
23. S. I. Han, S. Aramata, K. Yasuda, K. Kataoka, MafA stability in pancreatic β cells is regulated by glucose and is dependent on its constitutive phosphorylation at multiple sites by glycogen synthase kinase 3. *Mol. Cell. Biol.* **27**, 6593–6605 (2007).
24. C. Xu, N. G. Kim, B. M. Gumbiner, Regulation of protein stability by GSK3 mediated phosphorylation. *Cell Cycle* **8**, 4032–4039 (2009).
25. P. Lopez-Bergami, E. Lau, Z. Ronai, Emerging roles of ATF2 and the dynamic AP1 network in cancer. *Nat. Rev. Cancer* **10**, 65–76 (2010).
26. K. H. Goss, J. Groden, Biology of the adenomatous polyposis coli tumor suppressor. *J. Clin. Oncol.* **18**, 1967–1979 (2000).
27. M. M. Taketo, W. Edelmann, Mouse models of colon cancer. *Gastroenterology* **136**, 780–798 (2009).
28. H. Nagase, Y. Miyoshi, A. Horii, T. Aoki, M. Ogawa, J. Utsunomiya, S. Baba, T. Sasazuki, Y. Nakamura, Correlation between the location of germ-line mutations in the APC gene and the number of colorectal polyps in familial adenomatous polyposis patients. *Cancer Res.* **52**, 4055–4057 (1992).
29. J. Jen, S. M. Powell, N. Papadopoulos, K. J. Smith, S. R. Hamilton, B. Vogelstein, K. W. Kinzler, Molecular determinants of dysplasia in colorectal lesions. *Cancer Res.* **54**, 5523–5526 (1994).
30. E. R. Fearon, Molecular genetics of colorectal cancer. *Annu. Rev. Pathol.* **6**, 479–507 (2011).
31. K. M. Haigis, K. R. Kendall, Y. Wang, A. Cheung, M. C. Haigis, J. N. Glickman, M. Niwa-Kawakita, A. Sweet-Cordero, J. Sebolt-Leopold, K. M. Shannon, J. Settleman, M. Giovannini, T. Jacks, Differential effects of oncogenic K-Ras and N-Ras on proliferation, differentiation and tumor progression in the colon. *Nat. Genet.* **40**, 600–608 (2008).
32. P. H. Rooney, A. Boonsong, M. C. McFadyen, H. L. McLeod, J. Cassidy, S. Curran, G. I. Murray, The candidate oncogene *ZNF217* is frequently amplified in colon cancer. *J. Pathol.* **204**, 282–288 (2004).
33. S. Hidaka, T. Yasutake, H. Takeshita, M. Kondo, T. Tsuji, A. Nanashima, T. Sawai, H. Yamaguchi, T. Nakagoe, H. Ayabe, Y. Tagawa, Differences in 20q13.2 copy number between colorectal cancers with and without liver metastasis. *Clin. Cancer Res.* **6**, 2712–2717 (2000).
34. A. M. Carothers, S. H. Javid, A. E. Moran, D. H. Hunt, M. Redston, M. M. Bertagnolli, Deficient E-cadherin adhesion in C57BL/6J-Min/+ mice is associated with increased tyrosine kinase activity and RhoA-dependent actomyosin contractility. *Exp. Cell Res.* **312**, 387–400 (2006).
35. O. J. Sansom, V. Meniel, J. A. Wilkins, A. M. Cole, K. A. Oien, V. Marsh, T. J. Jamieson, C. Guerra, G. H. Ashton, M. Barbacid, A. R. Clarke, Loss of Apc allows phenotypic manifestation of the transforming properties of an endogenous K-*ras* oncogene in vivo. *Proc. Natl. Acad. Sci. U.S.A.* **103**, 14122–14127 (2006).
36. M. Raman, W. Chen, M. H. Cobb, Differential regulation and properties of MAPKs. *Oncogene* **26**, 3100–3112 (2007).
37. D. M. Owens, S. M. Keyse, Differential regulation of MAP kinase signalling by dual-specificity protein phosphatases. *Oncogene* **26**, 3203–3213 (2007).
38. K. P. Hoeflich, J. Luo, E. A. Rubie, M. S. Tsao, O. Jin, J. R. Woodgett, Requirement for glycogen synthase kinase-3β in cell survival and NF-κB activation. *Nature* **406**, 86–90 (2000).
39. S. A. Matheny, C. Chen, R. L. Kortum, G. L. Razidlo, R. E. Lewis, M. A. White, Ras regulates assembly of mitogenic signalling complexes through the effector protein IMP. *Nature* **427**, 256–260 (2004).
40. H. Niv, O. Gutman, Y. Kloog, Y. I. Henis, Activated K-Ras and H-Ras display different interactions with saturable nonraft sites at the surface of live cells. *J. Cell Biol.* **157**, 865–872 (2002).
41. M. R. Larsen, T. E. Thingholm, O. N. Jensen, P. Roepstorff, T. J. Jørgensen, Highly selective enrichment of phosphorylated peptides from peptide mixtures using titanium dioxide microcolumns. *Mol. Cell. Proteomics* **4**, 873–886 (2005).
42. A. E. Moran, D. H. Hunt, S. H. Javid, M. Redston, A. M. Carothers, M. M. Bertagnolli, Apc deficiency is associated with increased Egfr activity in the intestinal enterocytes and adenomas of C57BL/6J-Min/+ mice. *J. Biol. Chem.* **279**, 43261–43272 (2004).

Acknowledgments: We thank J. Chung for helpful discussion related to the roles of the regulation of Ras stability concerning physiology. We also thank J. Woodgett, M. A. White, R. C. Sears, T. Hagen, and Y. I. Henis for providing reagents. **Funding:** This work was supported by grants from the National Research Foundation (NRF), funded by the Ministry

Downloaded from stke.sciencemag.org on April 18, 2012

of Education, Science, and Technology of Korea through the Translational Research Center for Protein Function Control (2009-0083522); Mid-career Researcher Program (2010-0026844); and the Stem Cell Research Project number 2010-0020235. This work was also partly supported by a grant from the Ministry of Knowledge Economy [through the Korea Research Institute of Chemical Technology (SI-095)]. W.-J.J., J.Y., J.-C.P., S.K., Soung-Hoon Lee, and Seung-Hoon Lee were supported by a BK21 studentship from the NRF. **Author contributions:** W.-J.J., J.Y., and K.-Y.C. designed the study. W.-J.J., J.Y., J.-C.P., Soung-Hoon Lee, and S.K. performed the experiments. Seung-Hoon Lee and J.-B.Y. analyzed LC-MS/MS data. H.K. provided well-characterized patient samples. K.-Y.C. wrote the manuscript with contributions from W.-J.J. and J.Y. **Competing interests:** The authors declare that they have no competing interests. **Data and materials availability:** Use of the plasmids, p-Ras, and peptide requires a materials transfer agreement (MTA). W.-J.J. and K.-Y.C. are listed as inventors in a pending patent application associated with the p-Ras antibody and peptide described in this study.

Submitted 1 June 2011
Accepted 23 March 2012
Final Publication 10 April 2012
10.1126/scisignal.2002242
Citation: W.-J. Jeong, J. Yoon, J.-C. Park, S.-H. Lee, S.-H. Lee, S. Kaduwal, H. Kim, J.-B. Yoon, K.-Y. Choi, Ras stabilization through aberrant activation of Wnt/β-catenin signaling promotes intestinal tumorigenesis. *Sci. Signal.* **5**, ra30 (2012).

Downloaded from stke.sciencemag.org on April 18, 2012